Josephson Tunneling of Excited States in a Double-Well Potential

H. Susanto and J. Cuevas

Abstract We study the dynamics of matter waves in an effectively one-dimensional Bose–Einstein condensate in a double well potential. We consider in particular the case when one of the double wells con nes excited states. Similarly to the known ground state oscillations, the states can tunnel between the wells experiencing the physics known for electrons in a Josephson junction, or be self-trapped. Numerical existence and stability analysis based on the full equation is performed, where it is shown that such tunneling can be stable. Through a numerical path following method, unstable tunneling is also obtained in different parameter regions. A coupled-mode system is derived and compared to the numerical observations. The validity regions of the two-mode approximation are discussed.

1 Introduction

One fundamental physical phenomenon observable on a macroscopic scale is the Josephson tunneling of electrons between two superconductors connected by a weak link, predicted by Josephson in 1962 [1]. It is due to the macroscopic wave

H. Susanto (&)
School of Mathematical Sciences, University of Nottingham,
University Park, Nottingham, NG7 2RD, UK
e-mail: Hadi.Susanto@nottingham.ac.uk

J. Cuevas
Grupo de Física No Lineal, Departamento de Física Aplicada I,
Escuela Politénica Superior, Universidad de Sevilla,
C/ Virgen de Africa, 7, 41011 Sevilla, Spain

Progress Optical Sci., Photonics (2013): 583–599
DOI: 10.1007/10091_2012_11

Published Online: 2 August 2012

functions with global phase coherence that have a small spatial overlap. The first observation of this effect was reported by Anderson et al. [2].

Since the only requirement for the occurrence of Josephson tunneling is a weak coupling, [3] other weakly connected macroscopic quantum samples were also expected to admit such tunneling. For neutral superfluids, Josephson tunneling has been observed in liquid ^{3}He [4] and ^{4}He [5]. In the context of Bose–Einstein condensates (BECs) [6–12], the prediction was made by Smerzi et al. [13–15], followed by the experimental observation where a single [16, 17] and an array [18] of short Bose–Josephson junctions (BJJs) were realized. The idea of BJJs has also been extended to a long BJJ [19, 20], which mimics long superconducting Josephson junctions. Such a junction can be formed between two parallel quasi one-dimensional BECs linked by a weak coupling. Atomic Bose–Josephson vortices (BJVs) have also been proposed in [19, 20]. The solutions are akin to Josephson fluxons in superconducting long Josephson junctions [21] due to the relative phase of the solitons that has a kink shape with the topological phase difference equal to π. Moreover, it was emphasized that a BJV can transform from and to a dark soliton, due to the presence of a critical coupling at which the two solitonic structures exchange their stability [22]. In addition to BJVs that can be considered as domain-walls in the phase field, recently it is shown in [23] that a similar linearly coupled system may also admit solutions whose density difference forms a kink shape, i.e. the solutions are domain walls in the density field.

The study of Josephson tunneling in BECs considers the tunneling of the Thomas-Fermi cloud, i.e. a continuation of the ground state. The tunneling dynamics has been explained using a two-mode approximation [13–15]. The validity of the approximation has been shown in [24, 25]. To improve the applicability regime of such an approximation, modified coupled-mode equations have been presented in, e.g. [26–30].

It is important to note that in addition to the ground state, nonlinear excitations, such as dark matter waves, can also be created in BECs. Dark soliton dynamics in BECs with single well potentials has been studied theoretically (see reviews [31, 32]) and experimentally [33–35, 37]. Interesting phenomena on the collective behavior of a quantum degenerate bosonic gas, such as soliton oscillations [34–36] and frequency shifts due to soliton collisions [37] were observed. The evolution of solitons is of particular interest as the extent to which their behavior can be described in a particle picture is an open question and merits further experimental and theoretical investigation. A combination of soliton physics with the dynamics at weak links within double well potentials will shed light on the collective behavior of excited Bose–Einstein condensates in non-trivial potentials. In this paper, we present an analysis of the dynamics of dark matter waves in a double well potential. Static properties of such a configuration have been recently studied in [38, 39]. Here, we show that dark matter waves can also experience stable quantum tunneling between the wells. This implies that localized excitations in higher dimensions, such as vortices, may also experience Josephson tunneling. The (in)stability is obtained using numerical Floquet analysis. The numerical calculations are necessary as the stability of the observed tunneling is not immediately obvious. This is especially

the case because dark solitons are higher-order excited states. The possibility that modes with lower energy will be excited is not ruled out by a coupled-mode approximation.

The present paper is outlined as follows. In Sect. 2, we discuss the governing equation used in the current study. We then solve the equation numerically, where we obtain stable and unstable Josephson tunneling through a numerical path following method. The stability analysis is performed through calculating the Floquet multipliers of the solutions. In Sect. 3, we derive a coupled-mode approximation describing the tunneling dynamics. Good agreement between the numerics and the approximation is obtained and shown. We also discuss the failure of the coupled-mode approximation in capturing unstable Josephson tunneling. Finally we conclude the work in Sect. 4.

2 Josephson Tunnelings

2.1 Mathematical Model

We consider the normalized nonlinear Schrödinger (NLS) equation modelling the BECs (see, e.g., [40] for the scaling)

$$i\psi_t + \psi_{xx} + s|\psi|^2\psi - V(x)\psi = 0, \tag{1}$$

where ψ is the bosonic field, and t and x is the time and position coordinate, respectively. The parameter $s = \pm 1$ characterizes the attractive and repulsive nonlinear interaction, respectively, and $V(x)$ is the external double well potential, which for simplicity is taken as

$$V = \frac{1}{2}\Omega^2(|x| - a)^2, \tag{2}$$

with the parameters Ω and a controlling steepness and position of the two minima. The total number of atoms N in the trap is conserved with

$$N = \int_{-\infty}^{+\infty} |\psi|^2 dx. \tag{3}$$

Throughout the present paper, we set $s = -1$, i.e. we consider repulsive interactions between particles.

For non-interacting particles ($s = 0$) in a single well potential ($a = 0$), the governing equation (1) can be solved analytically to yield $\psi_n = e^{-iE_n t}\phi_n(x)$, where ϕ_n satisfies

$$\phi_{n+1} = \left(\frac{\Omega}{\sqrt[4]{2}}x - \frac{\sqrt[4]{2}}{\Omega}\partial_x\right)\phi_n, \quad n = 0, 1, 2, \ldots, \tag{4}$$

with

$$\phi_0 = e^{-\frac{\Omega}{2\sqrt{2}}x^2},$$

and the chemical potential E_n is given by

$$E_n = \frac{1}{2}\sqrt{2}(2n+1)\Omega.$$

The excitations ϕ_n can be continued to nonzero κ, which has been considered in, e.g., [41–51] (see also [52] for discussions on stationary solutions of the NLS equation with a multi-well potential that do not reduce to any of the eigenfunctions of the linear Schrödinger problem). Similar numerical continuations for localized modes in two-dimensional settings have been presented in, e.g., [53, 54]. The existence and the stability analysis of continuations of ϕ_n in a double-well potential has been discussed in [55], where it was shown that there is a symmetry breaking of the corresponding solutions, i.e. a change of stability from a symmetric to an asymmetric state. One typical manifestation of the instability is a periodic transfer of atoms between the wells, i.e. Josephson tunneling.

As most of Josephson tunneling studied in BECs considers the tunneling of a ground state cloud, which is a continuation of ϕ_0, here we consider in particular the tunneling of dark solitons as continuations excited states ϕ_1.

2.2 Numerical Periodic Solutions

To look for time-periodic solutions describing Josephson tunneling, we seek solutions that fulfills the relation $\psi(x,T) = \psi(x,0)$, with T being the period of the Josephson oscillations. Such solutions posses double periodicity, i.e. one due to the solitonic nature with a period $2\pi/E$, where E is the chemical potential (intra-well oscillations) and the other one caused by the Josephson effect (inter-well oscillations). Consequently, we can express the solutions in terms of a Fourier series multiplied by a factor related to the stationary character of dark solitons

$$\psi(x,t) = \exp(-iEt)\sum_{k=-\infty}^{\infty} z_k(x)\exp(ik\omega t), \tag{5}$$

where $\omega = 2\pi/T$ is the Josephson oscillation frequency. These solutions are denoted as commensurate if the commensurability condition $E = (q/p)\omega = (2q\pi)/(pT)$ is fulfilled, with $\{q,p\} \in \mathbb{N}$. In what follows, we fix $p = 1$.

Commensurate solutions are consequently fixed points of the map $\psi(x,0) \to \psi(x,T)$ and can be found either by using shooting methods in real space or algebraic methods in Fourier space. In order to do that, we will transform the problem into a discrete one by means of a finite difference discretization with spatial step $\Delta x = 0.2$ and apply the techniques developed for discrete breathers in Klein–Gordon lattices [56, 57]. If a shooting method were used, a time step $\Delta t = 0.02$ would be necessary. As the considered oscillations herein have periods about 1,500 time units, this

method would imply many integration steps. In addition to that, the lack of an analytical Jacobian would also imply the necessity of the numerical determination of this matrix. These facts suggest the suitability of the proposed Fourier space method, which, apart from transforming the set of differential equations into an algebraic one, provides an analytical expression for the Jacobian.

Truncating the Fourier series at k_m, i.e. the maximum value of $|k|$, which has been chosen to be 9 in most of the calculations due to computational reasons, Eq. (1) yields a set of nonlinear equations with the kth component of the dynamical equation set given by

$$F_k(x) \equiv (E - \omega k) z_k + \partial_x^2 z_k - V(x) z_k - s \sum_{m=-k_m}^{k_m} \sum_{n=-k_m}^{k_m} z_m z_n z_{k-m+n} = 0. \quad (6)$$

We then obtain the following expression for each component of the Jacobian

$$\begin{aligned} \frac{\partial F_k(x)}{\partial z_n(x')} = & \left\{ [E - \omega k - V(x)] \delta(x - x') + \partial_{xx}^2 \right\} \delta_{k,n} \\ & - s \delta(x - x') \sum_m \left[z_m^* z_{k-n+m} + z_m (z_{k-m+n} + z_{n+m-k}^*) \right], \end{aligned} \quad (7)$$

where we have written $z_k \equiv z_k(x)$ in both equations.

Once a periodic solution, say $\Psi(x,t)$, is obtained, to study its (linear) orbital stability one needs to analyze the time evolution of a small perturbation $\xi(x,t)$ to $\Psi(x,t)$. The equation satisfied to leading order by $\xi(x,t)$ is

$$i\xi_t + \xi_{xx} - s(2|\Psi|^2 \xi + \Psi^2 \xi^*) - V(x)\xi = 0. \quad (8)$$

Then, the stability properties of commensurate solutions can be determined by means of a Floquet analysis. It is performed by diagonalizing the monodromy matrix $\mathcal{M}$ which is defined as

$$\begin{bmatrix} \mathrm{Re}(\xi(x,T)) \\ \mathrm{Im}(\xi(x,T)) \end{bmatrix} = \mathcal{M} \begin{bmatrix} \mathrm{Re}(\xi(x,0)) \\ \mathrm{Im}(\xi(x,0)) \end{bmatrix}. \quad (9)$$

The linear stability of the solutions requires that the monodromy eigenvalues (also called Floquet multipliers) must be at the unit circle (see, e.g., [56, 58, 59] for details). In order to get the monodromy with enough accuracy, the simulations must be performed using a time step around $dt = 0.001$.

We have calculated commensurate solitons for $\beta = 0.1$ and $a = 10$ using the method described above and analysed the stability of those solutions. Presented in the top panels of Fig. 1 are two periodic solutions that we obtained in a double well potential. The left and right panel respectively corresponds to Josephson tunneling and a transition to macroscopic quantum self-trapping, similarly to the dynamics of the ground state oscillations [13, 15].

In the middle panels of Fig. 1, we present the distribution of the Floquet multipliers of the two solutions depicted in the top panels in the complex plane. It

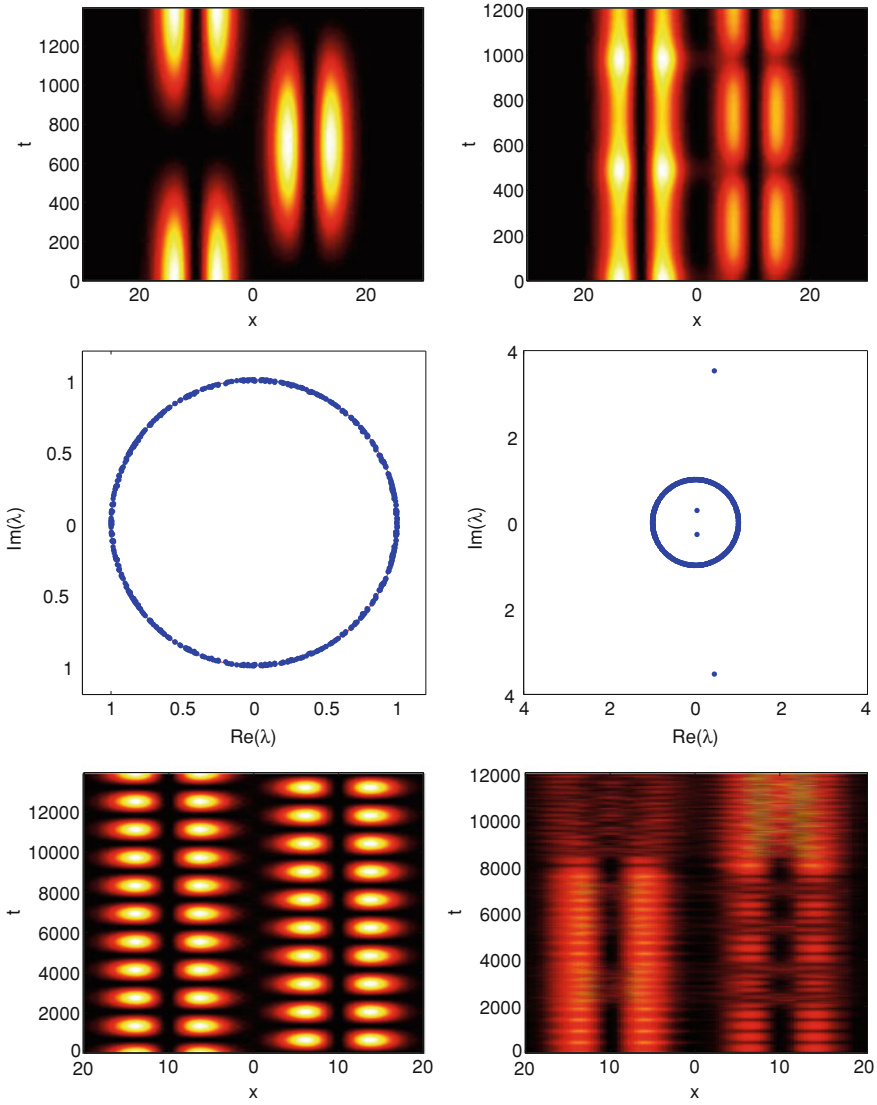

Fig. 1 (*Top*) The first few oscillations of the atom density $|\psi(x,t)|^2$ for dark solitons in a double well potential with $\Omega = 0.1$, $a = 10$, and (*left*) $\omega = 0.00450$ and (*right*) $\omega = 0.00520$, which respectively corresponds to $N = 0.0340$ and $N = 0.7677$. In both cases, the initial conditions are obtained from a numerical continuation with $\mu = 47$ (see the text). (*Middle*) Floquet multiplier distributions corresponding to solutions in the *top left and right panel*, respectively. (*Bottom*) Longer time evolutions of the *top panels* where one can see that the solution in the *top right panel* is indeed unstable

is worth noting that as there is a quartet of multipliers that do not lie on the unit circle, one can conclude that the solution in the top right panel is unstable.

We show in the bottom panels of Fig. 1 a longer time evolution of the solutions in the top panels, where one can see that the solution in the top right panel is indeed unstable. The instability we reported here is a clear evidence that the nonlinearity term in the governing equation (1) plays an important role, as all the solutions would have been stable otherwise. A typical instability dynamics is a repulsive interaction between the dark solitons in different wells so that they start to oscillate about the minimum of the wells as shown in the bottom right panel of Fig. 1. This is a typical dynamics due to the presence of complex eigenvalues, i.e. oscillatory instabilities.

We have also obtained periodic solutions for various parameter values. In the top left panel of Fig. 2 we show the dependence of the norm (number of atoms) N of tunneling dark solitons when the inter-well oscillation frequency is varied. In the panel, several representative values of q are considered. Note that the possible values of q are not limited to those shown in the graph. As ω is increased further, there is a critical value above which solutions are unstable. Unstable solutions are indicated as dashed lines in the top left panel. The solutions can also be continued for decreasing frequencies ω down to a critical value. Below this critical value, the only existing solutions are non-oscillating ones. In the top right panel of Fig. 2 we show the dependence of the growth rate (the logarithm of the maximum modulus of the Floquet multipliers) with respect to ω for $q = 47$. We also present the growth rate of Josephson tunneling for a fixed ω and q and variable separation distance between the two wells a in the bottom panels of the same figure, i.e. $\omega = 0.0049$ and $q = 47$. For small a, the solutions tend to a non-oscillating one with one dark soliton in each well, analogously to what occurs for small ω and fixed a.

3 Coupled-Mode Approximations and Their Validity

To describe dark soliton dynamics reported in the previous section, we will readily use a two-mode approximation derived in [27, 28]. Following [27, 28], we write

$$\psi = \sqrt{N}(b_2(t)\Phi_2(x) + b_3(t)\Phi_3(x)), \quad \Phi_{2,3} = \frac{\Phi_+(x) \pm \Phi_-(x)}{\sqrt{2}}, \tag{10}$$

where $\Phi_\pm(x)$ is a continuation of $\phi_{2,3}$ (4) for nonzero a satisfying

$$\partial_{xx}\Phi_\pm + \beta_\pm\Phi_\pm - V(x)\Phi_\pm + sN\Phi_\pm^3 = 0, \tag{11}$$

with the constraint $\int_{-\infty}^{+\infty} \Phi_j\Phi_k dx = \delta_{j,k},\ i,j = +,-$. Two examples of Φ_j, which corresponds to the norm N in the Fig. 1 are presented in Fig. 3. We obtained $\Phi_j(x)$ numerically by solving (11) using a fixed point algorithm, i.e. in this case a Newton–Raphson method.

Next, for simplicity we write $b_j(t) = |b_j(t)|e^{i\theta_j(t)}$. Equations (3) and (10) imply that $|b_2(t)|^2 + |b_3(t)|^2 = 1$. Defining

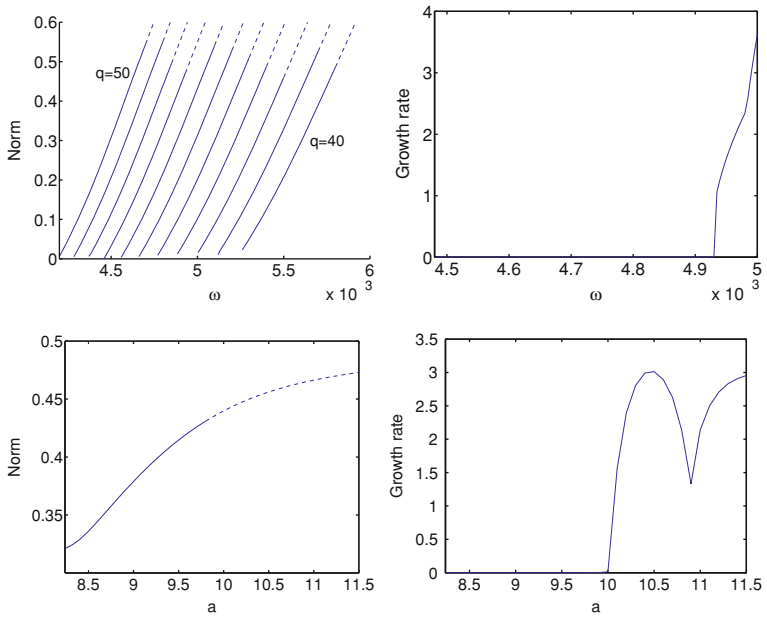

Fig. 2 The *top left panel* presents the dependence of the norm with respect to ω for dark solitons with $a = 10$. *Central panel* shows the minimum transmission coefficient for those solutions. *Dashed lines* indicate unstable solutions. Here q sweeps the values between 40 and 50. The *top right panel* shows the dependence of the growth rate with respect to ω for $q = 47$. *Bottom panels* depict the norm and the growth mode of tunneling dark solitons with fixed $\omega = 0.0049$ and $q = 47$ for varying a

$$z(t) = |b_2(t)|^2 - |b_3(t)|^2, \quad \Delta\theta(t) = \theta_3(t) - \theta_2(t), \tag{12}$$

one can obtain the equations satisfied by z and $\Delta\theta$ [27, 28]

$$\frac{dz}{dt} = -\frac{\partial H}{\partial \Delta\theta}, \quad \frac{d\Delta\theta}{dt} = \frac{\partial H}{\partial z}, \tag{13}$$

where

$$H = \frac{1}{2}Az^2 - B\sqrt{1-z^2}\cos\Delta\theta + \frac{1}{2}C(1-z^2)\cos 2\Delta\theta, \tag{14}$$

$$A = \frac{10\gamma_{+-} - \gamma_{++} - \gamma_{--}}{4}, \quad B = \beta_- - \beta_+ + \frac{\gamma_{++} - \gamma_{--}}{2}, \tag{15}$$

$$C = \frac{-2\gamma_{+-} + \gamma_{++} + \gamma_{--}}{4}, \tag{16}$$

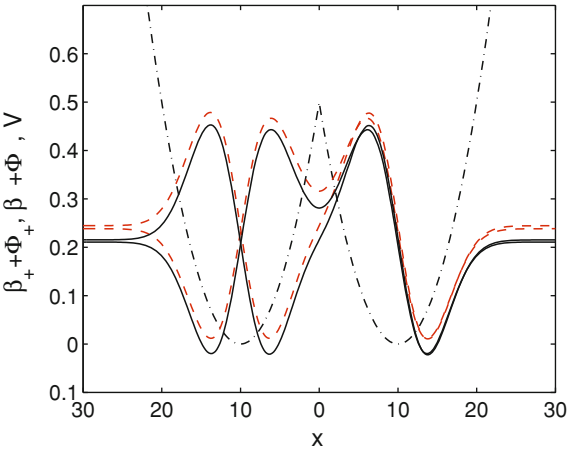

Fig. 3 The second and third collective modes of the con ning potential $V(x)$ (*dash-dotted*) for (*solid*) $N = 0.034$ and (*dashed*) $N = 0.7677$, with $s = -1$

$$\gamma_{jk} = -sN \int_{-\infty}^{\infty} \Phi_j^2(x)\Phi_k^2(x)dx, \tag{17}$$

with $j,k = +,-$. In the $(\Delta\theta, z)$-plane, Φ_+ and Φ_- correspond to the equilibrium point $(0,0)$ and $(\pm\pi, 0)$, respectively.

We plot the phase-portrait of (18) in Fig. 4 for the two values of N in Fig. 1. To compare the two-mode approximation with the top panels of Fig. 1, we calculate the variable z from the numerics of the full equation (1) as [27, 28]

$$z = \frac{\int_{-\infty}^{0} |\psi(x,t)|^2 dx - N/2}{NS}, \quad S = \left| \int_{-\infty}^{0} \Phi_+\Phi_- dx \right|,$$

where in the present case $S \approx 0.5$. As $\Delta\theta$ can be calculated immediately, one can compare the numerics and the approximation right away. Shown in Fig. 4 are the comparisons, where satisfactory agreement is obtained. The bold trajectory in the right panel is obtained from the top right panel of Fig. 1, i.e. only the first few oscillations are used such that the instability has not developed yet.

The phase portrait in the left panel of Fig. 4 has two families of periodic oscillations, i.e. one centred at $\Delta\theta = 0$ and the other at $\pm\pi$. The latter is known as π-oscillations [14]. The stable solution in the top left panel of Fig. 2 with $q = 50$ and the same norm belongs to this family. As for the phase portrait in the right panel of Fig. 4, one can also observe that there are two types of solutions, i.e. Josephson oscillations and running states. The latter type is also referred to as macroscopically quantum self-trapped states.

As for the instability of the solution in the top right panel that develops at a later time, it is clearly beyond the validity of the two-mode approximation presented herein. One would need a better ansatz for the approximation to capture the stability of the periodic solutions. We conjecture that the invalidity of the

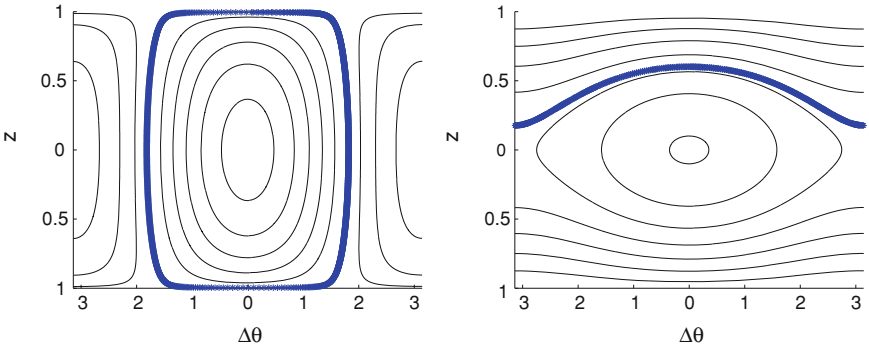

Fig. 4 The phase-portraits of (13) for the two values of N in Fig. 1, i.e. (*left*) $N = 0.0340$ and (*right*) $N = 0.7677$. *Thick symbols* correspond to the periodic solutions shown in the *top panels* of Fig. 1

approximation is caused by the assumption that the basis functions Φ_2 and Φ_3 are thought to be stable (time-independent), which are not necessarily the case. Note that the validity issue mentioned here is completely different from that in [27, 28]. In [27, 28], the issue is related to the fact that the approximation does not capture the Josephson oscillation of the full equation directly from the beginning, which typically occurs when $|sN| \gg 1$, while in our case $|sN| < 1$ and the approximation does capture the existence, but not the stability.

To analyse further the above conjecture, we have calculated the stability of the bases $\Phi_\pm$. The linear stability of Φ_j is determined by solving for the eigenvalues λ and eigenvectors $a(x)$ and $b(x)$ of the eigenvalue problem

$$\lambda a = \left(\beta_j + d_{xx} - V(x) + 2sN\Phi_j^2\right)a + sN\Phi_j^2 b,$$
$$-\lambda b = \left(\beta_j + d_{xx} - V(x) + 2sN\Phi_j^2\right)b + sN\Phi_j^2 a,$$

obtained by the substitution of

$$\psi(x,t) = \left[\sqrt{N}\Phi_j(x) + \epsilon\left(a(x)e^{i\lambda t} + b^*(x)e^{-i\lambda^* t}\right)\right]e^{-i\beta_j t}$$

into (1) and linearization in the formal small parameter ϵ. As the eigenvalues are generally complex, i.e. $\lambda = \lambda_r + i\lambda_i$, instability corresponds to $\lambda_i \neq 0$ due to the Hamiltonian structure of the equation. The stability analysis of the bases $\Phi_\pm$ as a function the norm N is summarized in Fig. 5.

From our numerical analysis, Φ_- becomes unstable at $N \approx 0.056$. At this point, a pair of eigenvalues bifurcates from the zero eigenvalues into the imaginary axis, i.e. an exponential instability. This change of stability is due to a symmetry-breaking (pitchfork) bifurcation with an asymmetric solution, which is accurately predicted by the two-mode approximation above (see, e.g. [36]). [Note that the equilibrium $(\Delta\theta, z) = (\pm\pi, 0)$ in the left and right panel of Fig. 4 has different stability. The stability does change at the critical norm above. The typical outcome

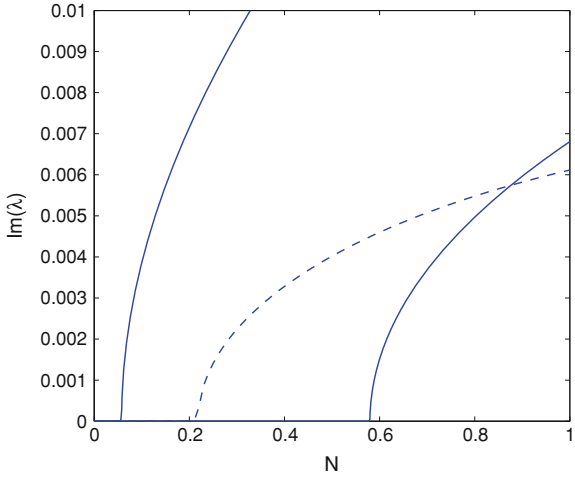

Fig. 5 The imaginary part of the unstable eigenvalues of Φ_+ (*dashed*) and Φ_- (*solid*) as a function of the norm N

of the instability is a stable time-periodic solution, which is in agreement with the two-mode approximation.

When N is increased further, there is a critical norm $N \approx 0.21$ above which Φ_+ becomes unstable. It is important to note that in this case the critical eigenvalue is complex, i.e. the solution suffers from an oscillatory instability, as shown in the top panel of Fig. 6 for $N = 0.3$. From the middle panel, it can be seen that the unstable mode creates out-of-phase oscillations of the dark soliton pairs in the wells. Computing the atom imbalance $z(t)$ and the phase-difference $\Delta\theta(t)$ between atoms in the wells, interestingly we obtain that the unstable dynamics still yields the equilibrium point $(\Delta\theta, z) = (0, 0)$. Another interesting observation is that superposing Φ_+ with Φ_- may suppress the instability provided that the coefficient of Φ_- is sufficiently large. As shown in the bottom panel of Fig. 6, even a coefficient as small as $\sqrt{0.1} \approx 0.32$ already reduces the instability of Φ_+. These may likely be related to the numerical results in Fig. 2, where we still obtained stable periodic solutions with norms slightly larger than $N = 0.3$.

Next, we increased N further and observed that for the stability of Φ_- there is a pair of complex eigenvalues that bifurcates in the complex plane at $N \approx 0.58$. The eigenvalue structure of the solution for $N = 0.7677$ is shown in the top panel of Fig. 7. Hence, in addition to an exponential instability, now Φ_- also suffers from an oscillatory instability. The typical dynamics of the state is presented in the middle panel, where initially the exponential instability creates partial tunneling of atoms from one well to the other followed by in-phase oscillations of the dark soliton pairs. As opposed to stabilization of Φ_+ due to a superposition of $\Phi_\pm$ when it becomes unstable, in the present case we did not observe any instability suppression. It may be because both Φ_+ and Φ_- are already unstable due to complex eigenvalues. This is also in agreement with the numerics in Fig. 2, where all the numerically obtained periodic solutions are unstable above $N \approx 0.58$ due to complex eigenvalues (see the middle, right panel of Fig. 1).

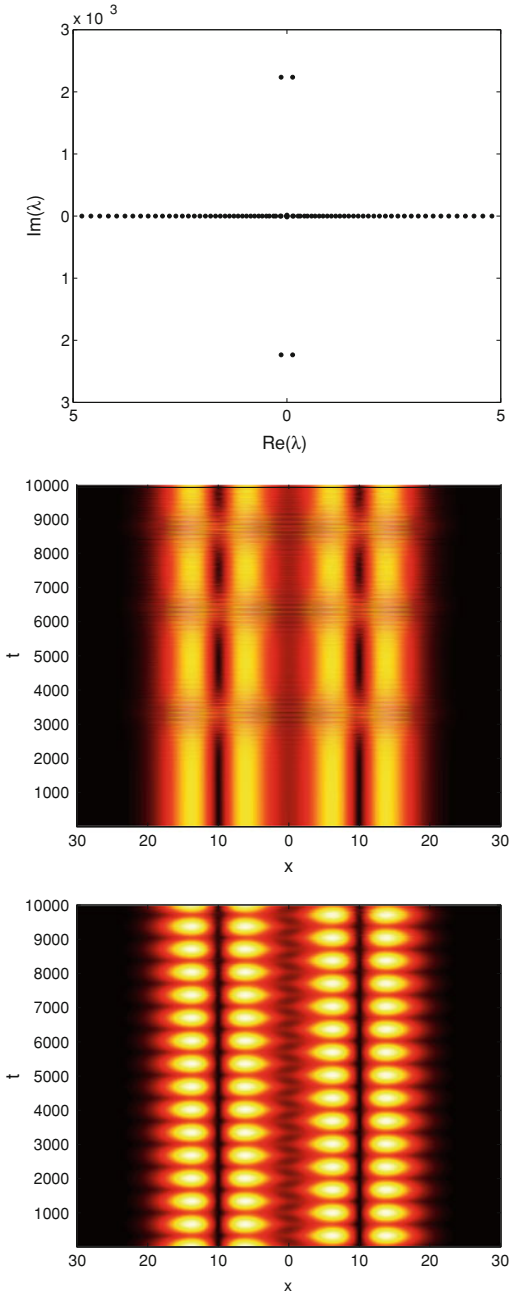

Fig. 6 (*Top*) The eigenvalue structure of Φ_+ for $N = 0.3$. (*Middle*) The dynamics of an unstable Φ_+ for the same norm. (*Bottom*) The dynamics of an initial condition $\psi(x, 0) = \sqrt{0.9}\Phi_+ + \sqrt{0.1}\Phi_-$

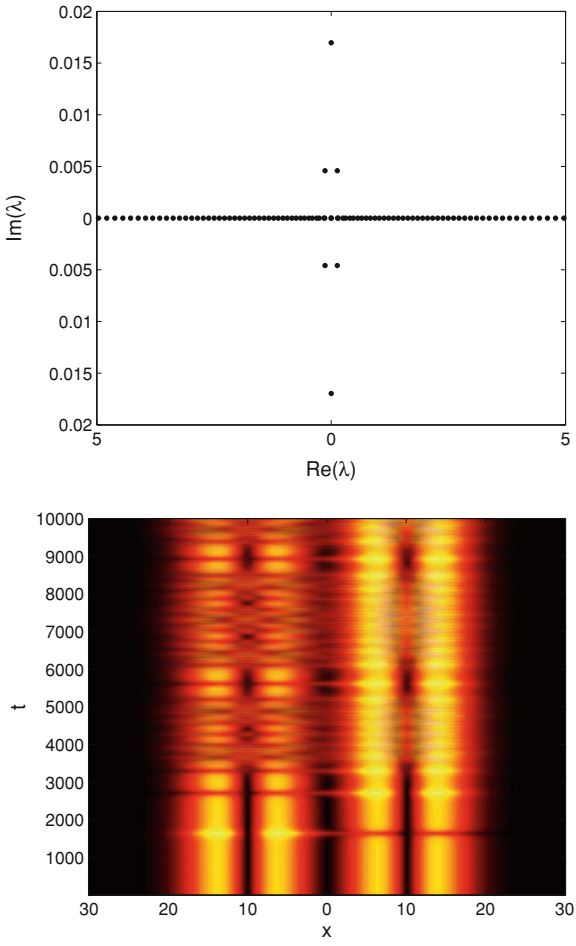

Fig. 7 The same as Fig. 6, but for Φ_- with $N = 0.7677$

4 Conclusion and Future Work

We have studied dynamics of excited states in a double well potential, where it has been shown that such states can experience tunnelings between the wells. Numerical stability analysis based on the full governing equation has been performed to show that the time-periodic solutions can be stable. Through path following methods, unstable solutions were also obtained. The instability is because of complex eigenvalues, i.e. oscillatory instability. A coupled-mode approximation has been derived to explain the numerical results. The break-down of the approximation has been discussed as well, where it was shown through a hand-wavy argument that two-mode approximations are not able to capture instability due to complex eigenvalues. Nevertheless, it was also shown trough numerical simulations that an instability caused by a quartet of complex eigenvalues can be

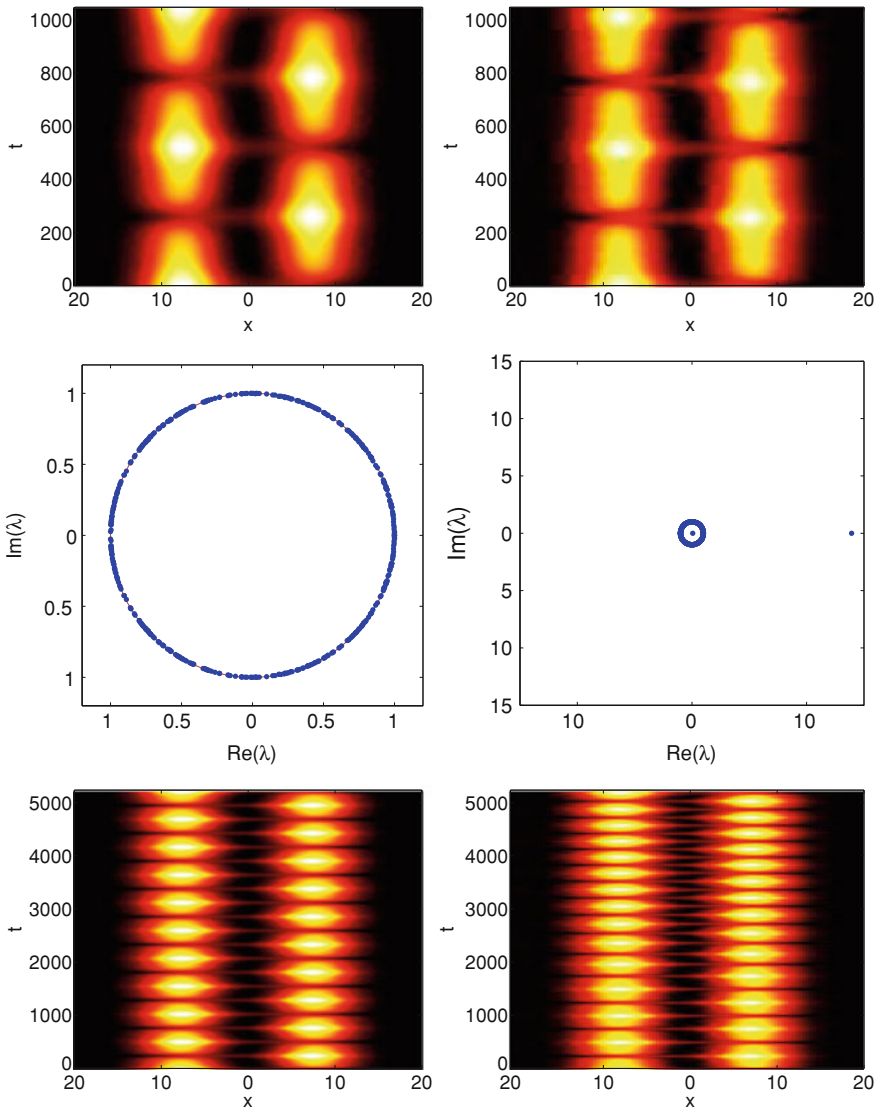

Fig. 8 (*Top*) The first two oscillations of the atom density $|\psi(x,t)|^2$ for a Thomas-Fermi cloud in a double well potential with $\Omega = 0.1$, $a = 7.5$, (*left*) $q = 10$ and (*right*) $q = 13$. In both cases, the initial conditions are obtained from a numerical continuation with $\epsilon = 0.01$. (*Middle*) Floquet multiplier distributions corresponding to solutions in the *top left and right panel*, respectively. (*Bottom*) Longer time evolutions of the *top panels* corresponding to 10 oscillation periods; clearly, the unstable solution develops oscillations with a period different from the initial one

suppressed by Josephson tunneling. In that regard, it is interesting to mention that the lifetime of purely black stationary solitons can be short due to quantum depletion [60], as atoms tunnel in to fill up the notch at the soliton center. In a

double-well potential, because the soliton dip can effectively tunnel from one well to the other and hence a periodic transfer of atoms in each well, Josephson tunneling may provide an alternative way to obtain a long-lived dark soliton by suppressing the depletion-induced decay of the soliton.

A natural problem to follow the analysis reported herein is the existence and stability of time-periodic solutions of the ground states (Thomas-Fermi cloud). A two-mode approximation for this case has been derived and discussed in, e.g., [27, 28]. Using the approximation, periodic solutions should be stable. We have performed preliminary computations presented in Fig. 8, where we also obtained unstable periodic solutions due to multipliers leaving at 1, i.e. exponentially unstable. Different from the dark soliton case, the instabilities here do not lead to the destruction of the periodicity of the solutions, but to a change in the oscillation period of the tunneling. Hence, again a coupled-mode approximation breaks down here. Nevertheless, our analysis presented above cannot be used in this case as the bases, which are continuations of ϕ_0 and ϕ_1 (see (4) and (11)), do not experience any oscillatory instability [55]. This is an ongoing work and will be reported elsewhere.

Several other directions that currently we work on include, on the one hand, the extension of the dark soliton tunneling to non-commensurate solutions using the technique developed in [61], and, on the other hand, an analysis of Josephson tunneling of excitations in polaritonic Bose–Einstein condensates [62] whose description includes gain and damping terms in the Gross–Pitaevskii equation [63].

Acknowledgments JC acknowledges nancial support from the MICINN project FIS2008-04848

References

1. B.D. Josephson, Phys.Lett. 1, 251 (1962)
2. P.L. Anderson, J.W. Rowell, Phys.Rev.Lett. 10, 230 (1963)
3. A. Barone, G. Paternò, *Physics and Applications of the Josephson Effect* (Wiley, New York, 1982)
4. S.V. Pereverzev, A. Loshak, S. Backhaus, J.C. Davis, R.E. Packard, Nature 388, 449 (1997)
5. K. Sukhatme, Y. Mukharsky, T. Chui, D. Pearson, Nature 411, 280 (2001)
6. S.N. Bose, Zeit. Phys. 26, 178 (1924)
7. A. Einstein, Sber. Preuss. Akad. Wiss. 22, 261–267 (1924)
8. A. Einstein, Sber. Preuss. Akad. Wiss. 1, 3–14 (1925)
9. M.H. Anderson, J.R. Ensher, M.R. Matthews, C.E. Wieman, E.A. Cornell, Science 269, 198–201 (1995)
10. K.B. Davis, M.-O. Mewes, M.R. Andrews, van N.J. Druten, D.S. Durfee, D.M. Kurn, W. Ketterle, Phys. Rev. Lett. 75, 3969–3973 (1995)
11. C.C. Bradley, C.A. Sackett, R.G. Hulet, Phys. Rev. Lett. 75, 1687–1690 (1995)
12. F. Dalfovo et al., Rev. Mod. Phys. 71, 463–512 (1999)
13. A. Smerzi, S. Fantoni, S. Giovanazzi, S.R. Shenoy, Phys. Rev. Lett. 79, 4950 (1997)
14. S. Raghavan, A. Smerzi, S. Fantoni, S.R. Shenoy, Phys. Rev. A 59, 620–633 (1999)
15. S. Giovanazzi, A. Smerzi, S. Fantoni, Phys. Rev. Lett. 84, 4521 (2000)
16. M. Albiez, R. Gati, J. Folling, S. Hunsmann, M. Cristiani, M.K. Oberthaler, Phys. Rev. Lett. 95, 010402 (2005)

17. S. Levy, E. Lahoud, I. Shomroni, J. Steinhauer, Nature **449**, 579 (2007)
18. F.S. Cataliotti, S. Burger, C. Fort, P. Maddaloni, F. Minardi, A. Trombettoni, A. Smerzi, M. Inguscio, Science **293**, 843 (2001)
19. V.M. Kaurov, A.B. Kuklov, Phys. Rev. A **71**, 011601 (2005)
20. V.M. Kaurov, A.B. Kuklov, Phys. Rev. A **73**, 013627 (2006)
21. A.V. Ustinov, Physica D **123**, 315 (1998)
22. M.I. Qadir, H. Susanto, P.C. Matthews, J. Phys. B: At. Mol. Opt. Phys. **45**, 035004 (2012)
23. N. Dror, B.A. Malomed, J. Zeng, Phys. Rev. A **84**, 046602 (2011)
24. A. Sacchetti, SIAM J. Math. Anal. **35**, 1160–1176 (2003)
25. A. Sacchetti, J. Evol. Eq. **4**, 345–369 (2004)
26. E.A. Ostrovskaya, Y.S. Kivshar, M. Lisak, B. Hall, F. Cattani, D. Anderson, Phys. Rev. A **61**, 031601–4 (2000)
27. D. Ananikian, T. Bergeman, Phys. Rev. A **73**, 013604 (2006)
28. D. Ananikian, T. Bergeman, Phys. Rev. A **74**, 039905(E) (2006)
29. X.Y. Jia, W.D. Li, J.Q. Liang, Phys. Rev. A **78**, 023613 (2008)
30. B. Juliá-Díaz, J. Martorell, M. Melé-Messeguer, A. Polls, Phys. Rev. A **82**, 063626 (2010)
31. V.V. Konotop, in *Emergent Nonlinear Phenomena in Bose–Einstein Condensates Theory and Experiment*, ed. by P.G. Kevrekidis, D.J. Frantzeskakis, R. Carretero-González (Springer, Berlin, 2008), pp. 65–97
32. D.J. Frantzeskakis, J. Phys. A: Math. Theor. **43**, 213001 (2010)
33. S. Burger, K. Bongs, S. Dettmer, W. Ertmer, K. Sengstock, A. Sanpera, G.V. Shlyapnikov, M. Lewenstein, Phys. Rev. Lett. **83**, 5198 (1999)
34. C. Becker, S. Stellmer, P. Soltan-Panahi, S. Dörscher, M. Baumert, E-M. Richter, J. Kronjäger, K. Bongs, K. Sengstock, Nature Phys. **4**, 496 (2008)
35. A. Weller, J.P. Ronzheimer, C. Gross, J. Esteve, M.K. Oberthaler, D.J. Frantzeskakis, G. Theocharis, P.G. Kevrekidis, Phys. Rev. Lett. **101**, 130401 (2008)
36. G. Theocharis, A. Weller, J.P. Ronzheimer, C. Gross, M.K. Oberthaler, P.G. Kevrekidis, D.J. Frantzeskakis, Phys. Rev. A **81**, 063604 (2010)
37. S. Stellmer, C. Becker, P. Soltan-Panahi, E.-M. Richter, S. Dörscher, M. Baumert, J. Kronjäger, K. Bongs, K. Sengstock, Phys. Rev. Lett. **101**, 120406 (2008)
38. S. Middelkamp, G. Theocharis, P.G. Kevrekidis, D.J. Frantzeskakis, P. Schmelcher, Phys. Rev. A **81**, 053618 (2010)
39. R. Ichihara, I. Danshita, T. Nikuni, Phys. Rev. A **78**, 063604 (2008)
40. R. Carretero-González, D.J. Frantzeskakis, P.G. Kevrekidis, Nonlinearity **21**, R139 (2008)
41. J.A. Vaccaro, O. Steuernagel, B. Lorimer, ArXiv:cond-mat/0007233v1
42. M.P. Coles, D.E. Pelinovsky, P.G. Kevrekidis, Nonlinearity **23**, 1753–1770 (2010)
43. R.J. Dodd, J. Res. Natl. Inst. Stand. Technol. **101**, 545 (1996)
44. Yu.S. Kivshar, T.J. Alexander, S.K. Turitsyn, Phys. Lett. A **278**, 225 (2001)
45. V.I. Yukalov, E.P. Yukalov, V.S. Bagnato, Phys. Rev. A **56**, 4845 (1997)
46. C. Trallero-Giner, J.C. Drake-Perez, V. López-Richard, J.L. Birman, Physica B **237**, 2342 (2008)
47. P.G. Kevrekidis, V.V. Konotop, A. Rodrigues, D.J. Frantzeskakis, J. Phys. B: At. Mol. Opt. Phys. **38**, 1173 (2005)
48. G.L. Al mov, D.A. Zezyulin, Nonlinearity **20**, 2075 (2007)
49. D.A. Zezyulin, G.L. Al mov, V.V. Konotop, V.M. Pérez-García, Phys. Rev. A **78**, 013606 (2008)
50. R. D'Agosta, B.A. Malomed, C. Presilla, Laser Phys. **12**, 37–42 (2002)
51. R. D'Agosta, B.A. Malomed, C. Presilla, Phys. Lett. A **275**, 424–434 (2000)
52. R. D'Agosta, C. Presilla, Phys. Rev. A **65**, 043609 (2002)
53. D. Mihalache, D. Mazilu, B.A. Malomed, F. Lederer, Phys. Rev. A **73**, 043615 (2006)
54. G. Herring, L.D. Carr, R. Carretero-González, P.G. Kevrekidis, D.J. Frantzeskakis, Phys. Rev. A **77**, 023625 (2008)
55. G. Theocharis, P.G. Kevrekidis, D.J. Frantzeskakis, P. Schmelcher, Phys. Rev. E **74**, 056608 (2006)

56. J.L. Marín, S. Aubry, Nonlinearity **9**, 1501 (1996)
57. J. Cuevas, J.F.R. Archilla, F.R. Romero, J. Phys. A: Math. and Theor. **44**, 035102 (2011)
58. T.R.O. Melvin, A.R. Champneys, P.G. Kevrekidis, J. Cuevas, Physica D **237**, 551 (2008)
59. S. Aubry, Physica D **103**, 201 (1997)
60. J. Dziarmaga, K. Sacha, Phys. Rev. A **66**, 043620 (2002)
61. D. Yan, J.J. Chang, C. Hamner, M. Hoefer, P.G. Kevrekidis, P. Engels, V. Achilleos, D.J. Frantzeskakis, J. Cuevas, J. Phys. B: At. Mol. Opt. Phys. **45**, 115301 (2012)
62. A.S. Rodrigues, P.G. Kevrekidis, J. Cuevas, R. Carretero-Gonzlez, D.J. Frantzeskakis, in the present book
63. J. Cuevas, A.S. Rodrigues, R. Carretero-González, P.G. Kevrekidis, D.J. Frantzeskakis, Phys. Rev. B **83**, 245140 (2011)